Single-crystal Magnetic Properties of Lanthanide Complexes. Part IX.[1] Hexakis(antipyrine)dysprosium(III) Tri-iodide

By M. Gerloch * and D. J. Mackey, University Chemical Laboratories, Lensfield Road, Cambridge CB2 1EW

The principal and average magnetic moments of hexakis(antipyrine)dysprosium(III) tri-iodide (antipyrine is 2,3-dimethyl-1-phenyl-Δ^3-pyrazolin-5-one) have been measured in the temperature range 80—300 K. The results are interpreted within a point-charge crystal-field model incorporating the D_{3d} symmetry of these six-co-ordinate complexes. Calculations are performed within the $^6H_{15/2} + {}^6H_{13/2}$ free-ion states as basis, corrected for the effects of intermediate coupling. Selected calculations including the $^6H_{11/2}$ state make insignificant changes. Average and principal moments do not vary significantly with ρ_6, the sixth-order radial crystal-field integral, unlike g-values. Values for the fourth-order integral ρ_4 and for $A_2^{\circ}\langle r^2\rangle$, related to the second-order crystal-field potential are estimated as *ca.* 400 and 160 cm^{-1}, respectively, and quantitative uncertainties in these values are discussed.

We continue our studies of the magnetic properties of trigonally distorted octahedral lanthanide compounds of formula Ln(antip)$_6$I$_3$ (antip = antipyrine = 2,3-dimethyl-1-phenyl-Δ^3-pyrazolin-5-one) with the f^9 complex of dysprosium(III). As usual the crystal-field calculations use a point-charge model of D_{3d} symmetry appropriate for this isomorphous series.[2] The order in which we have investigated this series has been largely determined by the complexity and length of the calculations, the present f^9 system appearing late because of a fairly dense parking of highly degenerate states near ground. Table 1 lists the observed free-ion eigenvalues of the eight lowest states estimated from spectra of dysprosium chloride, ethyl sulphate, and double-nitrate. These levels have been fitted by Wybourne [3] to a two-parameter, intermediate-coupling model by least-squares and in Table 1 we also show the

TABLE 1

Eigenvalues and eigenvectors for lowest states of f^9

State	$^6H_{15/2}$	$^6H_{13/2}$	$^6H_{11/2}$	$^6H_{9/2}$	$^6F_{11/2}$
Energy	0	3498	5848	7598	
% Purity	93	96	92	92	93
State	$^6H_{7/2}$	$^6F_{9/2}$	$^6H_{5/2}$	$^6F_{7/2}$	
Energy	8975		10,140	10,930	
% Purity	92	86	92	90	

percentage purities of the associated eigenvectors derived from this treatment. The 16-fold degenerate ground-state also contains *ca.* 6% $^4I_{15/2}$. Most of our calculations have involved diagonalization of the two lowest states (30 × 30 matrix) corrected for intermediate coupling as in the Appendix. Further checks including the third state, $^6H_{11/2}$, and a 42 × 42 matrix, made no significant change in any calculated magnetic moment. For this reason and also because of computer time and store we have made no checks using any larger basis. As usual,[1] the point-charge crystal-field model is parameterized by the second-, fourth-, and sixth-order radial integrals ρ_2, ρ_4, ρ_6 and by the effective distortion angle θ, being the angle subtended by any Dy–O bond and the molecular triad.

EXPERIMENTAL

Powder susceptibilities and crystal anisotropies of Dy(antip)$_6$I$_3$ were measured in the temperature range 300—80 K by the Gouy and Krishnan ' critical torque ' methods, respectively. The results, corrected for the diamagnetic properties of the lutetium analogue,[4] are given in Tables 2 and 3. Interpolated principal molecular magnetic moments are given in Table 4. Procedures and calibrations are as in ref. 5.

TABLE 2

Experimental average magnetic susceptibilities of Dy(antip)$_6$I$_3$

T/K	$10^6\chi'_M$ / c.g.s.u. mol^{-1}	T/K	$10^6\chi'_{\%}$ / c.g.s.u. mol^{-1}
302·0	45,300	191·5	70,800
295·5	46,150	175·0	77,150
284·0	48,100	162·0	83,050
278·0	49,000	146·5	91,450
269·5	50,500	130·0	102,100
259·5	52,200	114·0	116,100
239·0	56,900	101·5	129,700
222·5	61,050	90·5	144,800
206·5	65,250		

TABLE 3

Experimental molecular anisotropies of Dy(antip)$_6$I$_3$

T/K	$10^6(\chi_\parallel - \chi_\perp)$ / c.g.s.u. mol^{-1}	T/K	$10^6(\chi_\parallel - \chi_\perp)$ / c.g.s.u. mol^{-1}
293·0	12,000	174·0	26,900
279·0	13,250	160·5	29,950
264·5	14,450	142·5	34,850
251·0	15,700	130·5	38,700
235·0	17,300	116·0	45,500
221·0	19,100	98·5	52,950
205·5	21,200	87·0	62,600
190·0	23,650		

Figure 1 shows an example of the energy levels of the D_{3d} crystal-field states of the free-ion $^6H_{15/2}$ ground-state as functions of the distortion angle θ. Curves are shown dotted on the left-hand side between θ values 45 and

[1] Part VIII, preceding paper.
[2] R. W. Baker and J. W. Jeffery, *Acta Cryst.*, 1969, A, XIV 16 (Stony Brook Internat. Union. Cryst. Abs. 1969); R. W. Baker, personal communication.
[3] B. G. Wybourne, *J. Chem. Phys.*, 1962, **36**, 2301.
[4] M. Gerloch and D. J. Mackey, *J. Chem. Soc.* (*A*), 1970, 3040.
[5] B. N. Figgis, M. Gerloch, J. Lewis, and R. C. Slade, *J. Chem. Soc.* (*A*), 1968, 2028.

50° in which region calculations were not performed for reasons of computing economy. There is a change

TABLE 4

Interpolated principal magnetic moments of $Dy(antip)_6I_3$

T/K	$\bar{\mu}$/B.M.	$\mu_{\parallel}$/B.M.	$\mu_{\perp}$/B.M.
302·0	10·46	11·31	10·02
295·5	10·45	11·32	10·00
284·0	10·45	11·35	9·99
278·0	10·44	11·34	9·96
269·5	10·43	11·36	9·95
259·5	10·42	11·36	9·91
239·0	10·43	11·42	9·91
222·5	10·43	11·45	9·88
206·5	10·39	11·44	9·82
191·5	10·42	11·51	9·83
175·0	10·40	11·54	9·78
162·0	10·37	11·55	9·75
146·5	10·35	11·56	9·70
130·0	10·30	11·54	9·68
114·0	10·28	11·55	9·61
101·5	10·26	11·52	9·58
90·5	10·24	11·51	9·54

in ground-state in this region from the E'_g level which persists through most of the angular range. Interaction between the two lowest E'_g states is slight as seen by

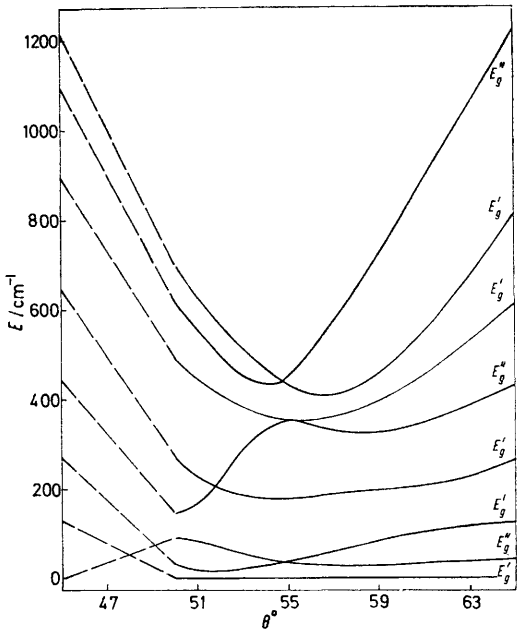

FIGURE 1 Energy levels of $^6H_{15/2}$ state of f^9 configuration as functions of θ. $\rho_2 = 1500$, $\rho_4 = 500$, $\rho_6 = 300$ cm^{-1}

the very close approach of these levels (*ca.* 20 cm^{-1}) at *ca.* 51·5°. The generally close packing of states near ground is responsible for the great length of the subsequent magnetic calculations which involve summing of the exponential terms over all populated states, *etc.* within the Van Vleck equation. Repulsion between all three E''_g states of $^6H_{15/2}$ is clearly large and is ultimately responsible for the change in ground-state at low angles. It is interesting to observe the constitution of the ground-state E''_g eigenvectors at $\theta = 45°$ as $|15/2, \pm 15/2\rangle$ when $g_{\parallel} = 20{\cdot}00$ and $g_{\perp} = 0{\cdot}00$.

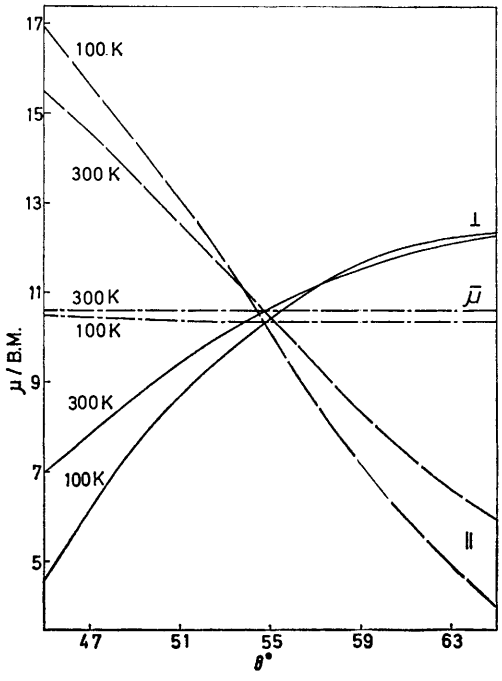

FIGURE 2 Principal and average moments of f^9 ions as functions of θ and temperature. $\rho_2 = 1500$, $\rho_4 = 500$, $\rho_6 = 300$ cm^{-1}

Principal and average magnetic moments are shown in Figure 2 as functions of θ. Their behaviour with respect to θ and temperature is what we have come to regard, in this series, as 'normal'. In particular,

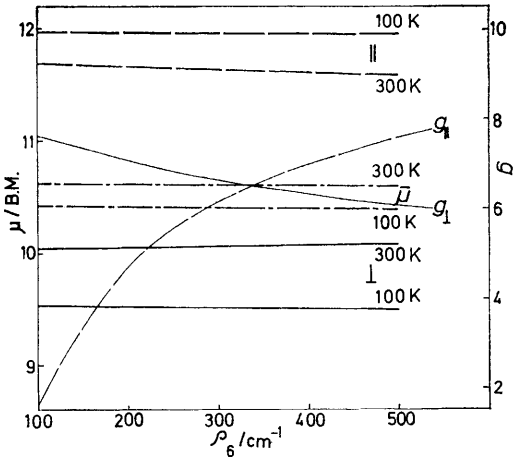

FIGURE 3 Principal and average moments of f^9 ions as functions of ρ_6: also principal g values. $\rho_2 = 1500$, $\rho_4 = 400$ cm^{-1}, $\theta = 53°$

$\bar{\mu}$(300 K) and $\bar{\mu}$(100 K) are approximately independent of the distortion angle θ and, not shown, of ρ_2. The temperature dependences of $\bar{\mu}$ and of anisotropies

$\Delta\mu$ are fairly small. The sign of anisotropy, determined by the sense of trigonal distortion, is such that $\mu_{\parallel} > \mu_{\perp}$ for $\theta < \theta_{oct}$.

All moments are remarkably insensitive to ρ_6 as shown in Figure 3, particularly the mean moments $\bar{\mu}$. This is somewhat surprising as the sixth-order crystal-field potential terms can operate within the $J = 15/2$ ground-state. That such terms do operate within this state is shown dramatically by the g values also plotted in Figure 3. As ρ_6 varies from 100 to 500 cm^{-1}, for example, $g_{\parallel}$ increases from 1·6 to 7·5. Similarly the sign of the g-value anisotropy Δg is clearly a sensitive function of ρ_6. Magnetic moments, $\bar{\mu}$ or $\Delta\mu$, are obviously no indication of ρ_6 values in this f^9 system so that e.s.r. information would be most desirable. Rubins [6] detected

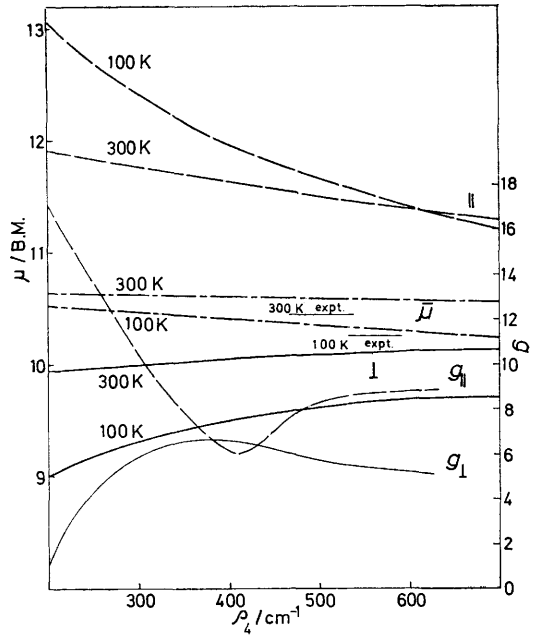

FIGURE 4 Principal and average moments and g values of f^9 ions as functions of ρ_4. $\rho_2 = 1500$, $\rho_6 = 300$ cm^{-1}, $\theta = 53°$. Experimental average moments for $Dy(antip)_6I_3$ as shown by horizontal lines.

several broad and extremely weak resonances in pure $Dy(antip)_6I_3$ at 20 and 4·2 K which were ' highly anisotropic ' but these may be spurious since, in a later paper, Baker and Rubins [7] report that no signals could be detected in this complex.

Figure 4 shows principal and average moments as functions of ρ_4. $\bar{\mu}$(300 K) Varies little with ρ_4 but $\bar{\mu}$(100 K) varies sufficiently to allow an estimate of ρ_4 to be made. While the principal moments $\mu_{\parallel}$ and $\mu_{\perp}$ vary smoothly with ρ_4, the principal g values again show complex behaviour and the sign of Δg can vary with ρ_4 as with ρ_6. In parenthesis, we note here that, while the results in Figures 3 and 4 were calculated with the $^6H_{15/2} + {}^6H_{13/2}$ basis, inclusion of the $^6H_{11/2}$ makes virtually no difference to the calculated μ or g values.

The experimental mean moments at 300 and 100 K are shown in Figure 4 from which it appears that no fit to $\bar{\mu}$(300 K) is possible for $\rho_4 < 1500$ cm^{-1} or more—a value which must be considered unacceptable by comparison with other members of this series. We must allow, however, for an experimental error of *ca.* 1—1·5% in the absolute values of $\bar{\mu}$, although we can rely more on their temperature variation. Fitting the temperature dependence of mean moments, *i.e.* $\bar{\mu}$(300 K) − $\bar{\mu}$(100 K), suggests ρ_4 *ca.* 400 cm^{-1} at which value absolute mean moments calculate *ca.* 1·5% too high. (Note the magnitude of these dysprosium moments in Figure 4.) This appears to be the best we can do bearing in mind the independence of $\bar{\mu}$ on θ, ρ_2, ρ_6, or larger basis.

Accordingly we use $\rho_4 = 400$ cm^{-1} (and a nominal ρ_6 value for computational purposes) and proceed with fitting anisotropies $\Delta\mu$ in the usual way. There is some temperature dependence of θ^f, the θ value chosen to fit $\Delta\mu$ for a given ρ_2 value, being in the sense θ^f(100 K) $< \theta^f$(200 K) $< \theta^f$(300 K) by *ca.* 1° for $\rho_2 = 500$ cm^{-1}. This temperature dependence nearly vanishes for $\rho_2 = 1000$—1500 cm^{-1} and reverses at $\rho_2 = 2000$ cm^{-1} when $\delta\theta$ (*i.e.* $|\theta^f(300) - \theta^f(100)|$) is *ca.* 0·05°. In Table 5

TABLE 5

$Dy(antip)_6I_3$: values of ρ_2, θ, and $A_2^{\circ}\langle r^2\rangle$ to fit anisotropies

$\rho_4 = 400$ cm^{-1}	($\rho_6 = 300$ cm^{-1})	$A_2^{\circ}\langle r^2\rangle = 3/2\ \rho_2\ (3\cos^2\theta - 1)$
T/K	θ°	$A_2^{\circ}\langle r^2\rangle$/$cm^{-1}$
$\rho_2 = 500$ cm^{-1}		
300	50·00	179
200	49·54	198
100	49·06	217
$\rho_2 = 1000$ cm^{-1}		
300	52·56	163
200	52·44	172
100	52·51	168
$\rho_2 = 1500$ cm^{-1}		
300	53·33	156
200	53·26	164
100	53·35	155
$\rho_2 = 2000$ cm^{-1}		
300	53·70	154
200	53·62	166
100	53·75	147

we present values of θ and $A_2^{\circ}\langle r^2\rangle$ for a family of ρ_2 values which fit experimental $\Delta\mu$ values exactly. For ρ_2 in the range $1000 < \rho_2 < 200$ cm^{-1}, $A_2^{\circ}\langle r^2\rangle$, being related to the second-order term in the crystal-field potential, takes on an essentially constant value of 160 ± 15 cm^{-1}, which value is also virtually independent of temperature. As usual, for $\rho_2 = 500$ cm^{-1} the $A_2^{\circ}\langle r^2\rangle$ value is a little larger.

[6] R. S. Rubins, 1961, D.Phil. Thesis, University of Oxford.
[7] J. M. Baker and R. S. Rubins, *Proc. Phys. Soc.*, **1961**, **78**, 1353.

For interest, we have recalculated the figures in Table 5 for $\rho_4 = 650$ cm^{-1} corresponding to the best compromise fit of the absolute values of $\tilde{\mu}$(300 K) and $\tilde{\mu}$(100 K) in which we 'sacrifice' the temperature dependence of $\tilde{\mu}$. Generally we find $A_2^{\circ}\langle r^2\rangle$ values are now *ca.* 230 ± 30 cm^{-1} for $1000 < \rho_2 < 2000$ cm^{-1} or 290 ± 40 cm^{-1} for $\rho_2 = 500$ cm^{-1}. Further, the temperature dependence of θ^f values is now 2—4 times greater than for $\rho_4 = 400$ cm^{-1}. For reasons already given, we consider the latter value of ρ_4 to be much more reliable and so report for Dy(antip)$_6$I$_3$; $\rho_4 = 400$ cm^{-1}, $A_2^{\circ}\langle r^2\rangle = 160$ cm^{-1}, ρ_6 indeterminate.

APPENDIX

Correction factors [8], by which crystal-field reduced matrix elements used in conjunction with pure Russell–Saunders state functions must be multiplied, have been calculated using the published eigenvectors.[3] They are as follows:

$U2$ $U4$ $U6$	$^6H_{15/2}$	$^6H_{13/2}$	$^6H_{11/2}$	$^6H_{9/2}$	$^6H_{7/2}$	$^6H_{5/2}$
$^6H_{15/2}$	0·9740 0·9867 0·9356					
$^6H_{13/2}$	0·9581 0·9642 0·9408	0·9615 0·9723 0·9638				
$^6H_{11/2}$	2·1956 0·6018 1·0839	0·8428 1·1206 0·5403	1·0067 13·7648 0·4504			
$^6H_{9/2}$	0 0·9899 1·0034	0·9430 0·9405 0·9414	0·9419 0·8461 −36·1380	0·9930 0·8906 0·9324		
$^6H_{7/2}$	0 1·0330 1·0623	0 0·9722 0·9873	0·9729 0·9048 1·0675	0·9460 0·9373 0·8287	0·9990 0·9004 0·9472	
$^6H_{5/2}$	0 0 1·0980	0 0·9883 1·0196	0 0·9265 1·0270	0·9223 0·9133 0·9254	0·9806 0·9415 0·9648	0·9959 0·9458 0

We thank the S.R.C. for a research award (to D. J. M.).

[1/1563 *Received, August 26th,* 1971]

[8] M. Gerloch and D. J. Mackey, *J. Chem. Soc.* (*A*), 1971, 3372.